UC Davis
Research Reports

Title

Development of Eco-Friendly Ramp Control for Connected and Automated Electric Vehicles

Permalink

https://escholarship.org/uc/item/63r0f737

Authors

Wu, Guoyuan
Zhao, Zhouqiao
Wang, Ziran
et al.

Data Availability

The data associated with this publication are available at: https://doi.org/10.6086/D10M3D

Development of Eco-Friendly Ramp Control for Connected and Automated Electric Vehicles

| January 2020 | A Research Report from the National Center for Sustainable Transportation |

Guoyuan Wu, University of California, Riverside

Zhouqiao Zhao, University of California, Riverside

Ziran Wang, University of California, Riverside

Matthew Barth, University of California, Riverside

TECHNICAL REPORT DOCUMENTATION PAGE

1. Report No. NCST-UCR-RR-20-04	2. Government Accession No. N/A	3. Recipient's Catalog No. N/A		
4. Title and Subtitle Development of Eco-Friendly Ramp Control for Connected and Automated Electric Vehicles		5. Report Date January 2020		
		6. Performing Organization Code N/A		
7. Author(s) Guoyuan Wu, Ph.D, https://orcid.org/0000-0001-6707-6366 Zhouqiao Zhao, https://orcid.org/0000-0002-5286-3807 Ziran Wang, Ph.D, https://orcid.org/0000-0003-2702-7150 Matthew J. Barth, Ph.D, https://orcid.org/0000-0002-4735-5859		8. Performing Organization Report No. N/A		
9. Performing Organization Name and Address University of California, Riverside Bourns College of Engineering – Center for Environmental Research & Technology 1084 Columbia Avenue Riverside, CA 92507		10. Work Unit No. N/A		
		11. Contract or Grant No. USDOT Grant 69A3551747114		
12. Sponsoring Agency Name and Address U.S. Department of Transportation Office of the Assistant Secretary for Research and Technology 1200 New Jersey Avenue, SE, Washington, DC 20590		13. Type of Report and Period Covered Final Report (October 2018 – September 2019)		
		14. Sponsoring Agency Code USDOT OST-R		
15. Supplementary Notes DOI: https://doi.org/10.7922/G23F4MWB Dataset DOI: https://doi.org/10.6086/D10M3D				

16. Abstract

With on-board sensors such as camera, radar, and Lidar, connected and automated vehicles (CAVs) can sense the surrounding environment and be driven autonomously and safely by themselves without colliding into other objects on the road. CAVs are also able to communicate with each other and roadside infrastructure via vehicle-to-vehicle and vehicle-to-infrastructure communications, respectively, sharing information on the vehicles' states, signal phase and timing (SPaT) information, enabling CAVs to make decisions in a collaborative manner. As a typical scenario, ramp control attracts wide attention due to the concerns of safety and mobility in the merging area. In particular, if the line-of-the-sight is blocked (because of grade separation), then neither mainline vehicles nor on-ramp vehicles may well adapt their own dynamics to perform smoothed merging maneuvers. This may lead to speed fluctuations or even shockwave propagating upstream traffic along the corridor, thus potentially increasing the traffic delays and excessive energy consumption. In this project, the research team proposed a hierarchical ramp merging system that not only allowed microscopic cooperative maneuvers for connected and automated electric vehicles on the ramp to merge into mainline traffic flow, but also had controllability of ramp inflow rate, which enabled macroscopic traffic flow control. A centralized optimal control-based approach was proposed to both smooth the merging flow and improve the system-wide mobility of the network. Linear quadratic trackers in both finite horizon and receding horizon forms were developed to solve the optimization problem in terms of path planning and sequence determination, and a microscopic electric vehicle (EV) energy consumption model was applied to estimate the energy consumption. The simulation results confirmed that under the regulated inflow rate, the proposed system was able to avoid potential traffic congestion and improve the mobility (in terms of average speed) as much as 115%, compared to the conventional ramp metering and the ramp without any control approach. Interestingly, for EVs (connected and automated EVs in this study), the improved mobility may not necessarily result in the reduction of energy consumption. The "sweet spot" of average speed ranges from 27–34 mph for the EV models in this study.

17. Key Words Connected vehicles, automated vehicles, ramp merging management, optimal control		18. Distribution Statement No restrictions.		
19. Security Classif. (of this report) Unclassified		20. Security Classif. (of this page) Unclassified	21. No. of Pages 41	22. Price N/A

Form DOT F 1700.7 (8-72) Reproduction of completed page authorized

NCST

About the National Center for Sustainable Transportation

The National Center for Sustainable Transportation is a consortium of leading universities committed to advancing an environmentally sustainable transportation system through cutting-edge research, direct policy engagement, and education of our future leaders. Consortium members include: University of California, Davis; University of California, Riverside; University of Southern California; California State University, Long Beach; Georgia Institute of Technology; and University of Vermont. More information can be found at: ncst.ucdavis.edu.

Disclaimer

Acknowledgments

Development of Eco-Friendly Ramp Control for Connected and Automated Electric Vehicles

A National Center for Sustainable Transportation Research Report

January 2020

Guoyuan Wu, Zhouqiao Zhao, Ziran Wang, and Matthew Barth

Center for Environmental Research & Technology, University of California, Riverside

NCST

[page intentionally left blank]

TABLE OF CONTENTS

List of Tables

List of Figures

Development of Eco-Friendly Ramp Control for Connected and Automated Electric Vehicles

EXECUTIVE SUMMARY

Connected and automated vehicle (CAV) technology has been widely developed during the past decade. With on-board sensors such as camera, radar, and Lidar, CAVs can sense the surrounding environment and be driven autonomously and safely by themselves without colliding into other objects on the road. In addition, CAVs are able to communicate with each other, and roadside infrastructure via vehicle-to-vehicle (V2V) and vehicle-to-infrastructure (V2I) communications, respectively, sharing information on the vehicles' states, signal phase and timing (SPaT) information. This enables CAVs to make decisions in a collaborative manner.

As a typical scenario, ramp control attracts wide attention from many researchers due to the concerns of safety and mobility in the merging area. In particular, if the line-of-the-sight is blocked (because of grade separation), then neither mainline vehicles nor on-ramp vehicles may well adapt their own dynamics to perform smoothed merging maneuvers. This may lead to speed fluctuations or even shockwave propagating upstream traffic along the corridor, thus potentially increasing the traffic delays and excessive energy consumption.

In this project, the research team proposed a hierarchical ramp merging system that not only allowed microscopic cooperative maneuvers for connected and automated electric vehicles (CAEVs) on the ramp to merge into mainline traffic flow, but also had controllability of ramp inflow rate, which enabled macroscopic traffic flow control. A centralized optimal control-based approach was proposed to both smooth the merging flow and improve the system-wide mobility of the network. Linear quadratic trackers in both finite horizon and receding horizon forms were developed to solve the optimization problem in terms of path planning and sequence determination, and a microscopic electric vehicle (EV) energy consumption model was applied to estimate the energy consumption. In addition, microscopic traffic simulation was conducted through PTV VISSIM to evaluate the impact of the proposed system on a representative highway segment of State Route 91 East (SR-91) in Corona, CA.

The simulation results confirmed that under the regulated inflow rate, the proposed system was able to avoid potential traffic congestion and improve the mobility (in terms of average speed) as much as 115%, compared to the conventional ramp metering and the ramp without any control approach. Interestingly, for electric vehicles (Connected and Automated Electric Vehicles in this study), the improved mobility may not necessarily result in the reduction of energy consumption. The "sweet spot" of average speed ranges from 27 mph to 34 mph for the EV models in this study.

Introduction

With the ever increase of travel demands, freeways play a significant role in facilitating the transportation-related activities. As an indispensable part of the freeway system, on-/off-ramps and the associated controls have attracted much attention from worldwide researchers for the following reasons:

- The ramp merging areas have consistently witnessed potential conflicts between on-ramp vehicles and mainline vehicles;
- Uncontrolled inflow traffic to the freeway network can lead to congestion;
- Due to limited vision range and uncoordinated merging behaviors with other vehicles, the drivers may experience unnecessary acceleration/deceleration, thus resulting excessive energy consumption and pollutant emissions.

Ramp metering is a widely used ramp merging management method, developed for conventional vehicles with human drivers. It utilizes the traffic signals installed on highway on-ramps to regulate the inflow rate of traffic entering the mainline according to prevailing mainline traffic conditions. Ramp metering usually consists of two-phase signal light (red and green only) together with a signal controller. For each green phase, one or more vehicles are allowed to enter the mainline, and the metering rate depends on the estimated traffic states in real time, such as lane occupancy, average speed, and length of on-ramp queue. This information is usually collected with fixed-location sensors, e.g., inductive loop detectors and cameras. Ramp metering is proved to be a cost-effective operational strategy to improve the safety, mobility and sustainability issue. The existing works have mainly fallen into three categories, namely rule-based approaches, control-based approaches, and learning-based approaches. However, since it inevitably introduces stop-and-go driving maneuver to the ramp vehicles, it often costs extra travel time and energy consumption of vehicles. Also, the ramp metering system leaves ramp vehicles much smaller room to adjust their speeds to merge into the mainline stream (due to mandatory stops at the meter), which potentially increases the safety risk.

On the other hand, connected and automated vehicle (CAV) technology has been studied extensively in the last decade. The idea of an automated vehicle based freeway system can be traced back to 1970 [1]. With the on-board sensing systems (such as radar, camera, LiDAR, ultrasonic, and even thermographic camera), CAVs can perceive the surrounding environment. With the communication abilities between CAVs and roadside infrastructures (i.e., vehicle-to-infrastructure communications) and among CAVs (i.e., vehicle-to-vehicle communications), detailed and accurate traffic information can be shared. Thus, higher resolution of system states can be estimated to improve the adaptability and system-wide optimality. Furthermore, the controllability of the automated vehicles enables the centralized or distributed coordination on the maneuvers of a number of vehicles for better performance. This may unlock abundant opportunities for more efficient and more delicate traffic management, including the ramp control.

Utilizing the CAV technique, many researchers have been trying to design a control system to cooperate vehicles' maneuvers in the ramp merging area to improve traffic efficiency. An extensive literature review is presented in the next Chapter. However, few ramp control approaches take the energy consumption into consideration when formulating the problem. Also, although the previous research proposed many sophisticated control methods, they failed to consider the entrance sequence of both mainline and ramp vehicles into the merging zone—the first-come-first-serve strategy and simplified estimated time of arrival (ETA) scheme are commonly used [2]. In addition, the cooperation of vehicles at merging area can only improve the local performance of the system. Unregulated inflow rate of the ramp vehicles can still lead to potential oversaturation the highway network, thus increasing the risk of upstream congestion and traffic accident around the merging area. To the authors' best knowledge, very few studies have focused on the energy efficient merging, not to mention the application of electric vehicle or more specifically connected and automated electric vehicles (CAEVs). It turns out to be a trade-off between mobility and environmental sustainability. Lastly, previous studies barely conducted microscopic traffic simulation. Their seemly sound results from numerical analysis under limited scope (e.g., a string of vehicles) may not represent long term impact on the dynamic traffic.

To address the aforementioned issue, we proposed a hierarchical system for corridor-wide ramp control, which solves the problem in three steps: a) corridor-wise ramp inflow rate determination; b) energy consumption-based sequence optimization; and c) individual vehicle trajectory optimization. More specifically, at the corridor level of the system, a cooperative protocol is introduced to calculate system-wide optimal inflow rate for each on-ramp, given the estimate of macroscopic traffic condition. The lower level controller coordinates the maneuvers of CAEVs locally at the ramp area and regulates the inflow rate accordingly. The proposed ramp merging control system first decides the set of vehicles to be controlled dynamically. Then the optimal merging sequence (involving both mainline and ramp vehicles) is identified, using a finite-horizon linear quadratic (LQ) tracker which predicts the optimal speed profiles in terms of energy consumption of the involved vehicles (both on-ramp and mainline) under specific conditions. With the identified optimal sequence, the vehicles are then controlled by a receding-horizon LQ tracker with the same parameters as the ones used in the prediction step. Finally, the next ramp leader vehicle (the first vehicle following the previous set of vehicles) is controlled to fit the suggested ramp inflow rate. It is noted that the energy consumption was estimated through a microscopic electric vehicle energy consumption model developed in our previous study [3].

Literature Review

In this chapter, we review a few aspects that are related to the development of proposed ramp control for Connected and Automated Electric Vehicles (CAEVs), including ramp metering strategy, cooperation among Connected and Automated Vehicles (CAVs), traffic state estimation, as well as driving behavior modeling.

Ramp Metering

A ramp meter is a traffic signal on a freeway on-ramp area that is used to regulate the inflow rate of vehicles onto the freeway. Although there are some review papers about ramp metering algorithms in the past few decades, such as [4]–[6], latest progress in this area especially related to machine learning technique was not included. In this section, we divide the up-to-date ramp metering algorithms into three categories: 1) rule-based; 2) control-based; and 3) learning-based, and review them, respectively.

Rule-based Approaches

A typical rule-based approach contains a hierarchy logic to adjust the ramp rate internally and coordinately. In general, the rule-based algorithms are easy to define, modify, and are relatively computational efficient. They simplify the nonlinear feature of the traffic, which is complex to be modeled accurately without hard assumptions.

A widely used rule-based method to achieve system-wide coordination is competitive approach, which usually contains two competitive controllers running in parallel, where the more restrictive metering rate would be chosen. Additional adjustment could be introduced to address other constrains like queue effects. Bottleneck Algorithm [7] used upstream occupancy and bottleneck data as system inputs, and the algorithm contains coordinated bottleneck controllers and local controllers. Similar to the Bottleneck Algorithm, two-module structure were proposed in the System-Wide Adaptive Ramp Metering (SWARM) Algorithm [8] as well. SWARM made decision based on estimated lane density using Kalman filter and linear regression. The local controller (called SWARM2) calculated metering rates by preserving headway which was converted from estimated local density, and the coordinated controller (called SWARM1) calculated metering rates to adjust the current density to the desired value.

ZONE [9] Algorithm was another well-known rule-based approach which segmented freeway into zones, and it used Conservation Law to model the volume change of the traffic. By integrating the real-time measurement on upstream mainline volume with historical data, the algorithm chose a predefined metering rate accordingly. Fuzzy Logic [10], [11] algorithm was developed in 1998, which converted empirical knowledge into finite fuzzy rules. The proper choice of rules might lead to a robust system, but it could be overwhelming to identify appropriate rules for a system-wide ramp metering. Advanced Real-time Metering System (ARMS) [12] was made up of free-flow control, congestion prediction, and congestion reduction. The algorithm maximized the throughput and tried to reduce the risk of congestion, and Origin-Destination (O-D) information was used to distribute the calculated ramp volume to each ramp. Dynamic Ramp Metering [13] is a hierarchical coordinated control of ramps that

contains state estimation, OD prediction, local control and area-wide control to minimize the total system travel time.

Control-based Approaches

Control-based approaches introduce automatic control techniques such as feedback control into the ramp metering system. Unlike the rule-based approaches whose strategies may be sophisticated, control-based ones are usually succinct, robust and efficient. However, the nonlinearity of the traffic dynamics poses some challenges for these approaches.

ALINEA was first proposed by Papageorgiou et al. [14] in 1991. By introducing the feedback into the control design, the algorithm is robust to the disturbance. Papageorgiou et al. also provided a guideline for the design of ALINEA ramp metering system [15]. The algorithm uses downstream occupancy as system inputs, controls the metering rates in response to the change of occupancy, and regulates them to the desired level. Although ALINEA is a local ramp metering algorithm, it draws much attention due to its simplicity, stability, and efficiency. Therefore, a large number of variations of ALINEA have been proposed to adapt to more complicated scenarios (e.g., METALINE, FL-ALINEA, UP-ALINEA, XALINEA/Q, PI-ALINEA) [5] [16]–[19] or to extend for achieving system-wide benefits (HERO) [20].

Linear-quadratic (LQ) feedback control algorithms are another type of control-based methods proposed by Isaksen and Payne [21] and Golstein and Kumar [22], which optimize the system performance such as throughput (vehicle miles per hour). In order to minimize total delay of the freeway network, Model Predictive control (MPC) approaches were applied by some researchers. Hegyi et al. [23] proposed a MPC scheme in a rolling horizon framework to coordinate the variable speed limits and ramp metering. To coordinate the traffic flows in an urban network with both freeways and arterial, Haddad et al. [24] developed an MPC-based algorithm for perimeter control including ramp metering strategies. Stratified Ramp Metering Algorithm was proposed by Geroliminis et al. [25], where a more accurate density estimation algorithm was developed. The metering rates were calculated to delay the onset of the breakdown and to accelerate system recovery. The algorithm could be regarded as an extended version of Stratified Zone Algorithm (SZM) [26] which aims to maximize the network throughput. The MPC scheme was also used to solve the optimization problem.

Learning-based Approaches

With the rapid advance in machine learning techniques such as artificial neural network (ANN) and reinforcement learning, more and more learning-based approaches for ramp metering emerge recently. Because of the nonlinear feature of traffic dynamics, learning-based approaches seem to be a shortcut to achieve better performance.

Zhang et al. proposed a local freeway ramp metering using ANN [27]. The controllers calculate the proportional-integral (PI) feedback gain using multi-layer feed-forward (MLF) neural network which can be tuned by both historical data and on-line streaming data. Coordinated Ramp metering algorithm using ANN was firstly proposed by Wei and Wu [28]. The coordinated metering rate was trained by a traffic simulation model and expert system.

The recent breakthroughs of Reinforcement Learning (RL) provide another promising direction for ramp metering. Numerous RL-based algorithms have sprung up in the past five years. A local ramp metering algorithm was developed by Lu and Huang [29]. Fares et al., and Lu et al. proposed a coordinated ramp metering algorithm using Q-Learning technique [30], [31]. Belletti et al. proposed an expert level ramp metering control based on multi-task deep reinforcement learning [32], and Schmidt-Dumont et al. combined ramp metering with variable speed limits based on decentralized reinforcement learning [33].

Coordination of CAVs

In this section, we mainly review the literature that were focused on the low-level system of the coordinated ramp control, which is the coordination of CAVs in terms of their motion control algorithms. Some previous work was reviewed by Rios-Torres et al. and Scarinci et al. [34], [35]. However, in this section, we strategically categorize all related literature into two types: centralized approaches and distributed approaches. Additionally, we include more recent papers that were not reviewed by the previous surveys.

Centralized Approaches

In this section, we define a CAV coordination approach as centralized if the tasks and control commands of the system are globally conducted by the roadside infrastructure and/or the transportation management center (TMC) for all CAVs. Some of the major reasons that such coordination is conducted in a centralized manner are that, each CAV in the system might not have global information of the system, nor can they conduct computations locally that consume large computational power and long computational time.

In some centralized approaches, tasks and control commands were executed by different layers of the centralized controller. A two-layer CAV coordination system at ramp was proposed by Schimidt et el. in 1983, which was based on non-linear system dynamics behavior [36]. In their system, the higher layer is in charge of the sequence control, while the lower layer is in charge of the motion control of vehicles. Ran et al. proposed a similar centralized multi-layer automated ramp system, and also built a microscopic simulation model to validate its characteristics, as well as the designing requirements of the minimum ramp length [37].

Other than aforementioned approaches, coordination of CAVs at ramp can also be modeled as an optimization problem to be solved by the centralized controller, with the aim of minimizing travel time or fuel consumption. Awal et al. proposed an optimization problem with the objective of reducing merging time at ramps and thus reducing merging bottlenecks [38]. Raravi et al. formulated an optimization problem which aims at minimizing the Driving-Time-To-Intersection (DTTI) of vehicles, subject to certain constraints for ensuring safety [39]. Rios-Torres et al. presented an optimization framework and an analytical closed-form solution that allowed online coordination of CAVs at on-ramp merging zones [2]. Xie et al. formulated this case as a nonlinear optimization problem, and conducted a simulation evaluation with MATLAB and Car2X module in VISSIM [40].

Distributed Approaches

Different from centralized approaches that rely on the roadside infrastructure and/or the TMC with infrastructure-to-vehicle (I2V) communication, distributed approaches of CAV coordination at ramp control conduct coordination decisions locally among different CAVs through vehicle-to-vehicle (V2V) communication. Compared to the centralized approaches, the distributed approaches bring several benefits, including reducing communication requirement and improving scalability.

The concept of virtual vehicle coordination at ramps was originated from Uno et al. [41]. The proposed approach maps a virtual vehicle onto the highway main line before the actual merging happens, allowing vehicles to perform safer and smoother merging maneuver. Lu et al. applied a similar idea in their proposed systems, where they first formulated the merging problems differently with respect to two different geometric layouts of the road (i.e., either with or without a parallel lane), and then proposed a speed based closed-loop adaptive control method to control the longitudinal speed of merging CAVs [42].

Besides the virtual vehicle ideas, other distributed approaches were also proposed to control the longitudinal motion of CAVs at ramps. Dao et al. proposed a distributed control protocol to assign vehicles into vehicle strings in the merging scenario [43]. Zhou et al. developed a vehicle trajectory planning method for CAV coordination at ramp, formulating the planning tasks of the ramp vehicle and the mainline vehicle as two related distributed optimal problems [44]. Wang et al. proposed a distributed consensus-based CAV coordination system [45]. Furthermore, agent-based modeling and simulation of the proposed CAV coordination system was conducted in game engine Unity, and it was compared to human-in-the-loop simulation to evaluate its benefits in terms of mobility and sustainability [46].

Traffic State Estimation

Accurate measurement and estimation of prevailing traffic conditions are the foundation of effective ramp control system, especially from the perspective of corridor-level coordination. Since it is difficult and expensive to obtain complete information on the traffic (e.g., 100% penetration rate of connected vehicles), estimation of traffic states, such as flow, density, and speed, from partially observed traffic data plays an important role. Seo et al. performed a comprehensive survey about traffic state estimation which provides a guideline into this field [47].

The categories listed below are on the basis of their suggestion. At the macroscopic scale, road networks are divided into several segments without further merging or diverging, which are called links. Inside each link, the traffic states can be considered to be homogeneous. Usually, flow (veh/hr), density (veh/km), and speed (km/hr) are three key variables used for traffic flow management. There might be other equivalent variables. For example, some ramp metering algorithms use occupancy as system input, which is quite comparable to density with the assumption or estimation of vehicle length. Raw data available for estimation can be categorized as: stationary and mobile. The stationary data is collected by fixed location sensors

such as inductive loop detectors, micro-wave radars on roadside, and surveillance cameras. The mobile data is collected by moving vehicles equipped with sensors such as GPS, on-board radar, and camera. The emergence of CAVs on roads can provide a significant amount of mobile sensor data.

Traffic flow model is widely used for traffic state estimation. The models are usually based on physical and empirical relations. Borrowing the idea of hydrodynamic theory, fundamental diagram depicts the relationship between density and speed, and/or density and flow [48–49]. Another dynamic representation model with the hydrodynamic theory is cell transmission model (CTM) [50], which utilizes the discrete analog of the differential equations arising from a special case of the hydrodynamic model of traffic flow. Because of the conservation law for the traffic hydrodynamic, the aggregated behavior of traffic is depicted by partial differential equations. Lighthill-Whitham-Richard (LWR) model is the most commonly used first-order model [51–52], and there are many higher-order models such as Payne-Whitham (PW) model [53–54].

Model-based Approaches

Model-based approaches are widely used in the field of traffic state estimation, where aforementioned traffic flow models are applied. The parameters of the models are usually calibrated via historical data from the field. After the calibration, target data is fed into the model to estimate the traffic states. Coifman proposed a method of estimating microscopic vehicle information (i.e., travel times and trajectories) using LWR model and loop detector data [55]. Wang and Papageorgiou estimated macroscopic traffic via Extended Kalman Filter (EKF) [56]. However, these approaches may fail if inappropriate models are adopted. Furthermore, as the parameters are calibrated by specific data sets, the model-based approaches may not be so adaptive to the drastic changes of traffic conditions.

Learning-based Approaches

Different from model-based approaches, no empirical traffic flow models are used in learning-based approaches. Learning-based models are trained through statistical methodologies or machine learning techniques given a large amount of historical data. A typical learning-based estimation approach was proposed by Tak et al. [57], in which k-nearest neighbors (KNN) algorithm was applied. Because of the challenge to well interpret the features of learning scheme, it is difficult to analytically comprehend how the entire system works even though the results may be very attractive. Additionally, similar to the model-based approaches, the dependency of trained data set makes the system not flexible enough to transfer to other untrained scenarios.

Streaming-data-driven Approaches

Without using neither empirical models nor historical data, streaming-date-driven approaches only rely on real-time data and "weak" assumptions. Therefore, it is more robust to different traffic conditions. The "weak" assumption such as Conservation Law is generally reasonable, considering the physical constraints. A recent research was performed by Florin et al. [58], who

presented mobile observer method with aggregated information of number of overtaking maneuver of vehicles. The increasing number of CAVs and connected vehicles on freeways can provide a large amount of streaming data for traffic state estimation, which makes it possible to consider mixed traffic scenarios. Bekiaris-Liberis el al. proposed a mixed traffic state estimation method with streaming-data-driven approach utilizing only average speed measurements reported by connected vehicles and a minimum number (sufficient to guarantee observability) of spot-sensor-based total flow measurements [59].

Driving Behavior

Although we assume full penetration rate of CAVs in this study[1], the review of human driving behavior may provide useful insight for the potential extension to mixed traffic scenarios.

Modeling and predicting the driving behavior of conventional human-driven vehicles are essential for designing the motion behavior of CAVs in mixed traffic conditions. As the foundation of microscopic traffic models, car-following (CF) logic describes the longitudinal interactions between vehicles assuming there is no lane changing or overtaking. Over the past decades, a considerable number of car-following models have been proposed and developed [60–61]. For instance, Gipps model [62], Krauss model [63] and intelligent driver model (IDM) [64] were well-developed to address the speed adjustment according to the principle of collision avoidance between vehicles. A comprehensive comparative study of car-following models used in the state-of-the-art microscopic traffic simulators was conducted in [65]. More recently, to improve the traffic flow stability, an anticipation optimal velocity model (AOVM) was proposed by Peng et al. considering the anticipation effect of optimal velocity [66]. Given that human factors plays an essential role in driving behaviors especially under complex traffic conditions, notable efforts have been made to integrate human factors into the conventional CF model in order to describe more realistic driving behavior [61]. For example, an adaptive neural-fuzzy inference system (ANFIS) was proposed in [67] that integrated human expert knowledge and neural network to adapt the vehicle speed for car-following and collision prevention. Instead of assuming constant reaction time, Khodayari et al. proposed an artificial neural network (ANN) car-following model to estimate the following vehicle's acceleration based on variable reaction delay input [68]. In [69], a number of numerical tests showed that ANNs provide a good approximation of car following dynamics. Comparative studies and evaluation between major car-following models under mixed traffic conditions can be found in [70].

To describe the driving behavior in various traffic situations, some new methods have been proposed that use mathematical models and neural networks like Bayesian filtering, Recurrent Neural Network to predict a driver's intended actions across traffic situations [71–72]. Artificial neural network (ANN) and radial basis function neural network (RBF-NN) showed great benefits to predict the vehicle second-by-second trajectory in congested traffic condition in terms of

---

[1] Out of the control zone (see Figure 1), the vehicles' dynamics are governed by the default car-following model of the simulation software in this study.

accuracy and efficiency [73–74]. To investigate the cause of stop-and-go pattern and estimate the vehicle behavior in traffic, Agamennoni et al. proposed a recursive Bayesian filtering approach for that purpose [71]. The problem of multi-agent inference was tackled by decoupling the joint inference to log-linear combinations of individual dependencies. Toledo et al. [75] further developed an integrated driving behavior model that combine lane changing behavior and acceleration based on target lane model and target gap model as short-term goal and plan.

Some cutting-edge research involved studying the interaction between human driven vehicle and CAVs. To investigate the impact of AVs on traffic flow, the authors in [76] assumed both AVs and human-driven vehicles follow the well-known intelligent driver model (IDM) but with different parameters. Simulation study of a single AV and several human-driven vehicles interaction showed with stabilization can be achieved via a single autonomous vehicle driving around the equilibrium speed [77]. In this work, a second-order car following model (i.e., optimal-velocity-follow-the leader model) was applied to describe the human-driven vehicles' behaviors as well as AV. With estimating vehicle behaviors and anticipate their future trajectories, more effective coordination between vehicles could be achieved in mixed traffic condition.

Problem Formulation and System Architecture

Problem Formulation

Figure 1 illustrates a typical highway-ramp merging area. However, different from the traditional ramp metering scenario which has a traffic light located at the end of the ramp, we consider the scenario with the following assumptions in this paper:

- All vehicles are CAEVs whose information (e.g., position, speed, and acceleration) are perfect and are shared via V2I or V2V communications. And their speeds can be fully controlled by the acceleration/deceleration signals sent from a centralized processor.
- There is no communication delay or package loss in either V2V or V2I communications.
- Once the affected mainline vehicles are selected by the merging algorithm, they will not change lanes to preserve the number of controlled vehicles, or overpass other mainline vehicles to disturb the entrance sequence into merging area.

With the appropriate control, it is expected that the involved CAEVs may avoid unnecessary stops (as mandatory by the ramp metering) before the completion of merging maneuvers, while the inflow rate on ramp or even the time headway between on-ramp vehicles can be well regulated.

Since we only control the longitudinal dynamics of the vehicles, we set up a one-dimensional coordinate system and map the positions of vehicles on both mainline and ramp to the system.

The dynamics of n vehicles in the proposed ramp merging system can be given by:

$$\dot{p}_i = v_i, \dot{v}_i = u_i \qquad (1)$$

where $i(\in [1,2,\dots,n])$ is the vehicle index; p and v represent the position and speed of the vehicle, respectively; and u denotes the acceleration of the vehicle, which acts as the input of the proposed system. If we define the overall system state as

$$x = \begin{pmatrix} p_1 \\ p_2 \\ \dots \\ v_1 \\ v_2 \\ \dots \\ v_n \end{pmatrix}, \text{ and the observation as } y = \begin{pmatrix} p_1 - p_2 \\ p_2 - p_3 \\ \dots \\ p_{n-1} - p_n \\ v_1 \\ v_2 \\ \dots \\ v_n \end{pmatrix}$$

the system can be written as the following linear form:

$$\dot{x} = Ax + Bu$$
$$y = Cx \tag{2}$$

where A is a $2n \times 2n$ system matrix of constant coefficients that describes the state transfer; B is a $2n \times n$ control matrix of the coefficients that weigh the inputs; and C is a $(2n - 1) \times 2n$ output matrix.
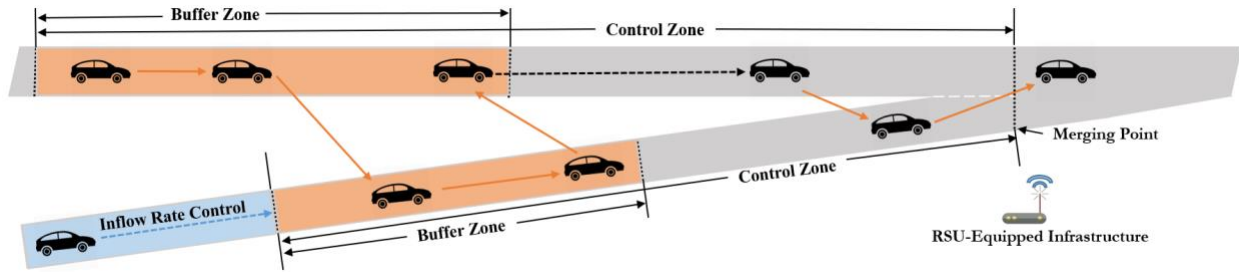
Figure 1. Illustration of different zones of the proposed optimal control-based ramp merging system.

Then, we formulate the optimization problem in the following quadratic form. The cost function is defined as the sum of the deviations of the measurements and control effort.

$$\min J = \frac{1}{2} \sum_{k=0}^{N-1} \{(y_k - r_k)^T Q(y_k - r_k) + u_k^T R u_k\} + \frac{1}{2}(y_N - r_N)^T Q(y_N - r_N)$$

$$s.t. \, x_{k+1} = Ax_k + Bu_k, \, y_k = Cx_k \tag{3}$$

$$Acc_{\min} \leq u_k \leq Acc_{\max}$$

$$((p_i)_k - (p_{i+1})_k) \geq Gap_{\min}$$

where r_i is the gap and speed reference to be tracked; Q and R matrices define the weights of the objective function to be tuned, respectively, for the system outputs and inputs. $[Acc_{\min}, Acc_{\max}]$ is a feasible input range that the vehicles can achieve. $Gap_{\min}$ is the hard safety constraint to avoid collision. In the simulation, $Acc_{\max}$ equals to $2.5m/s^2$; $Acc_{\min}$ equals to $-3m/s^2$; and $Gap_{\min}$ equals to 2s headway times initial speed v_{i0}. It is noted that herein we simplify the safety constraint by borrowing the concept for legacy vehicles. CAEVs may require more complex collision-free constraints (e.g., string stability issue for a platoon of CAEVs) or even shorter $Gap_{\min}$ than legacy vehicles (from an individual CAEV perspective) due to their quicker reaction times and better control capability. If vehicle i and vehicle $i+1$ are on the same lane (i.e., either both on the ramp or both on the mainline), this constraint should be held strictly. If vehicle i and vehicle $i+1$ are on different lanes (e.g., one on the mainline while the other on the ramp), this constraint need to be held when they arrive at (or very close to) the merging area.

Definition of Control Zone and Buffer Zone

To solve this problem, we first specify the roadway segment with two types of zones: control zone and buffer zone for the on-ramp and mainline, respectively, as shown in Figure 1. In the control zones of both mainline and on-ramp, a centralized processor is employed to receive and process the incoming information from CAEVs and send the control signals back to CAEVs to achieve system-wide energy efficiency. Buffer zones (in orange) are located on the upstream portion of the control zones, and are designed to continuously monitor the incoming vehicles and collect information to support subsequent control decision. As vehicle streams keep flowing into the network, control decision cycles (in time) are segmented and the involved CAEVs (with the consideration of regulated inflow rate) of each cycle are determined once the first unregulated vehicle hits the downstream boundary of the on-ramp buffer zone. By controlling the speed of each involved CAEV, the inter-vehicle gaps and traveling speed can be well regulated to ensure the safety at the merging zone. It is noted that if the number of vehicles within the on-ramp buffer zone exceeds the inflow rate to be regulated during the current cycle, then the partial of stream will be controlled and deferred to enter the merging area in the next cycle.

Figure 2 shows an example of the trajectories of vehicles in the system to illustrate how vehicles are controlled. The orange curves illustrate the vehicles' trajectories controlled by the optimal algorithm; The blue dash curves depict the predicted trajectories of the leading vehicles for the next control decision cycle without regulating the on-ramp inflow rates; The solid blue curves present the controlled trajectories of these leading vehicles with the compliance of the inflow rates; The yellow curves represent the trajectories of vehicles following the leading vehicles whose trajectories have been regulated for the sake of inflow rate (i.e., solid blue curves).

System Architecture

A typical freeway system contains multiple on-ramps and off-ramps. As mentioned in previous chapters, by leveraging CAV technology, we can better estimate and predict the traffic states in

real time, and develop a ramp control system that can: 1) improve the operational efficiency of entire freeway by cooperatively regulating the inflow rates of all ramps; 2) mitigate safety concerns at the ramp merging areas by coordinating the movements of vehicles on both mainline and ramp; and 3) reduce the excessive vehicular energy consumption and emissions by smoothing the longitudinal maneuvers of CAVs. If conventional human-driven vehicles are involved, design of the trajectories for CAVs should predict the behavior of conventional vehicles based on certain models such as car-following and merge gap acceptance. Figure 3 illustrates a generalized system architecture of the cooperative ramp control system for mixed traffic. As shown in the figure, the hierarchical system can be divided into a real-time data processor and a 3-level structure.
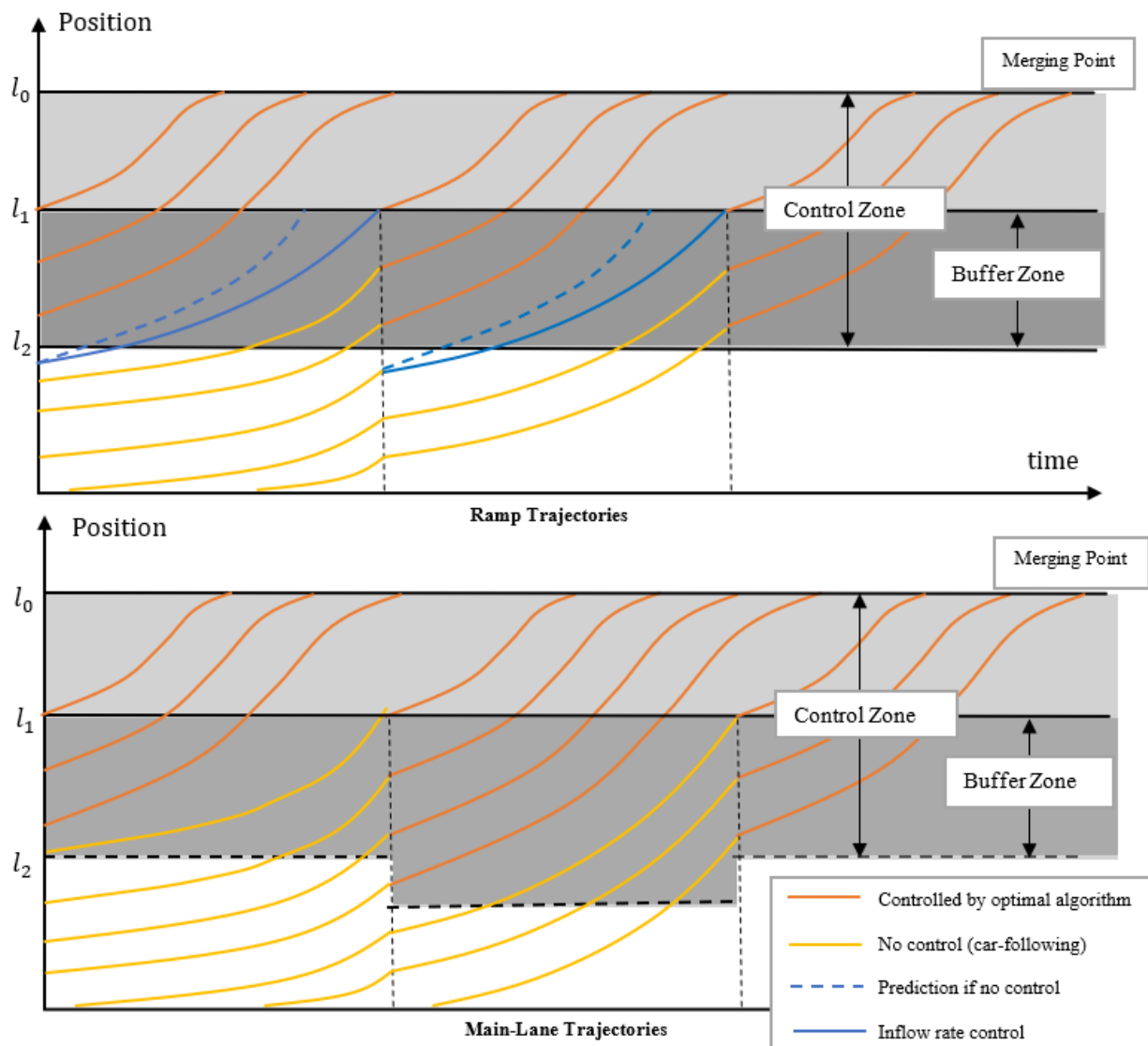

Figure 2. Illustration of the vehicle's trajectories on ramp and the mainline.

1) At the corridor-level, the ramp metering algorithm calculates system-wide optimal inflow rate for each on-ramp, given the estimate of macroscopic traffic states. The resultant inflow rate serves as the constraint for boundary control at lower level (i.e., ramp-level). It should be pointed out this strategy is applicable to homogeneous flow (either all legacy vehicles or all CAVs as considered in this study). For mixed traffic, the conventional ramp metering algorithms need to be further extended to consider CAVs in the context, where a hybrid ramp control strategy should be developed.

2) The ramp-level module coordinates the maneuvers of CAVs and human-driven vehicles at the merging area and regulates the ramp inflow rate based on the output from the corridor-level control. Desired CAVs trajectories are calculated by a centralized controller. To complete this task, the controller should keep tracking the human-driven vehicles and predicting their behaviors, and the trajectories of CAVs should be adjusted accordingly.

3) Once the trajectory is calculated for the involved CAV, a lower-level controller (at the vehicle dynamics level) is designed for trajectory tracking. Please note that the powertrain control of the CAVs is out of the scope of this study.
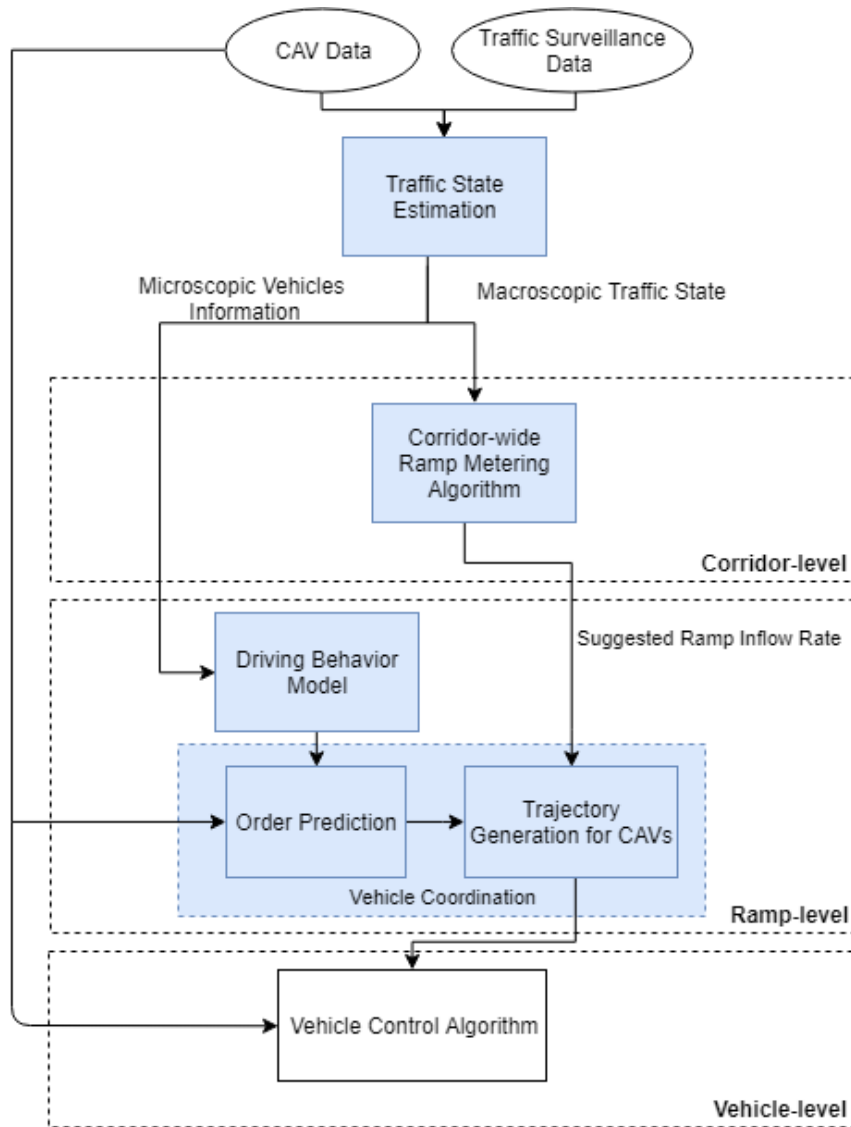
Figure 3. Illustration of the generalized system architecture.

Regarding the major blocks in Figure 3, extensive literature review has been performed and summarized in Chapter 2. Also, it should be pointed out that at the corridor-level control, we applied the Stratified Ramp Metering (SRM) Algorithm directly and determined the appropriate ramp metering rates. We put significant efforts into ramp-level and vehicle-level control. Figure 4 further elaborates the detailed flowchart for the ramp level and vehicle level control, with the external input suggested ramp inflow rate (i.e., determined by SRM).
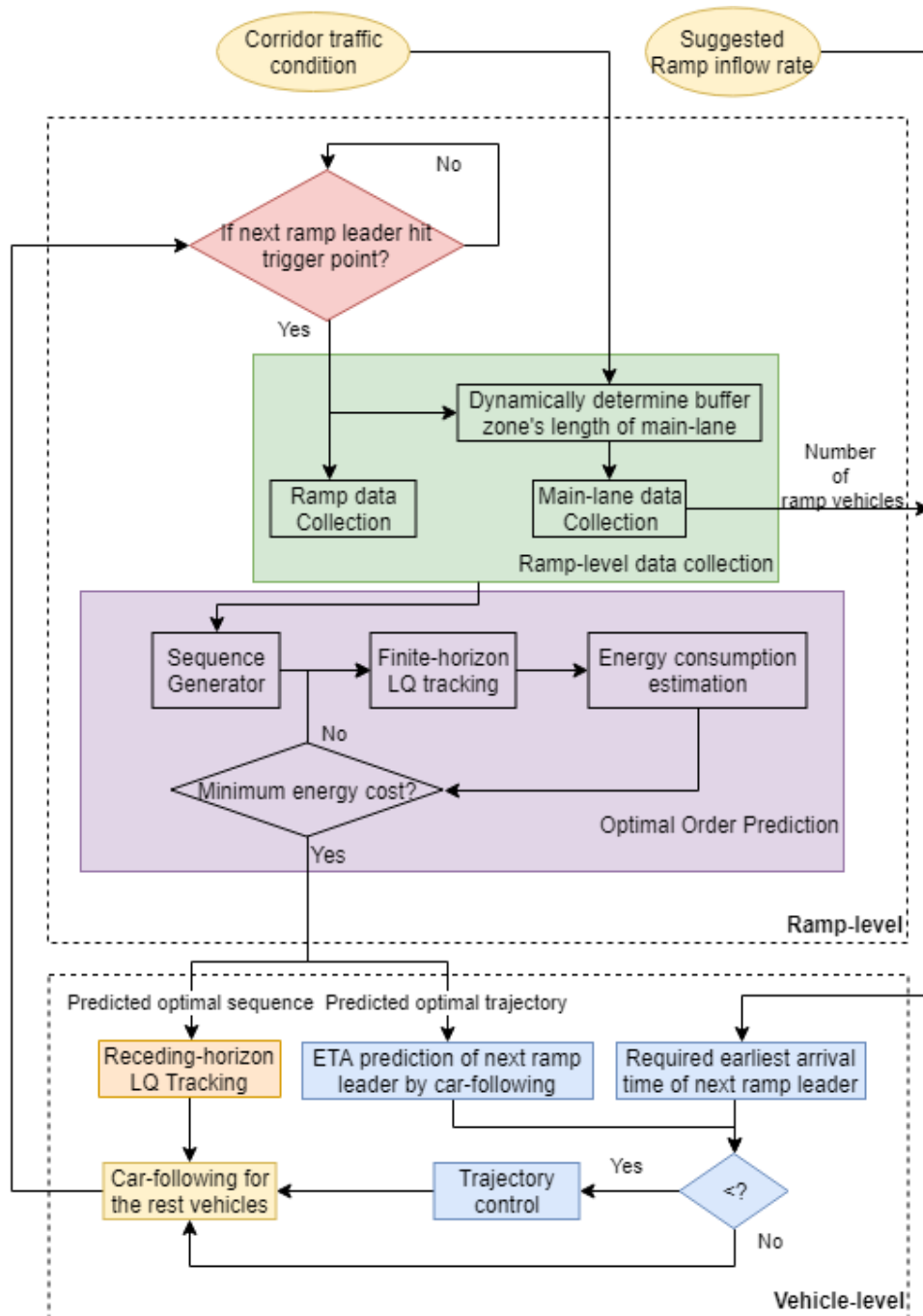
Figure 4. Flowchart of the proposed ramp-level and vehicle-level control.

1) *Ramp level*: data collection and vehicle merging sequence optimization. In the data collection module, vehicles' information (such as position, speed, and lane index) is collected once they enter the buffer zones. Usually, the ramp buffer zone is determined based on its physical length, while the length of the mainline buffer zone may vary with prevailing traffic conditions. Because the controller is designed to regulate the vehicles to form a compact string, it is important to know the entrance sequence of the vehicles into

![NCST logo]

the merging zone. Intuitively, the sequence would have impacts on the string-wise energy consumption. Instead of using a heuristic sequencing protocol, such as first-come-first-serve, we developed an optimal sequence determination module to identify the most energy efficient sequence. The module exams all possible sequences, applied the finite-horizon linear quadratic (LQ) tracker to predicting the controlled speed profile of each involved vehicle, estimated the associated energy consumption, and selected the least energy consumption sequence for the vehicle level control.

2) *Vehicle level*: motion control of individual vehicles. For the involved vehicles, the longitudinal motion controller is designed to be a receding horizon LQ tracker. To match the predicted energy consumption in the optimal sequence determination step, we use the same controller parameters as in the associated finite-horizon LQ tracker. Details of controller design will be presented in the Methodology chapter.

Methodology

In this chapter, we will discuss the detailed methodology for each key step in the flow chart of the proposed ramp control system (see Figure 4), including metering rate estimation, involved vehicle identification, optimal sequence determination, and vehicle motion control.

Metering Rate Estimation

At the corridor-level, the control algorithm calculates the system-wide optimal inflow rate for the on-ramp, given the measurement of macroscopic traffic states (such as flow, occupancy, and speed). The resultant inflow rate serves as the constraint for boundary control at the lower level (i.e., ramp-level). To implement such function, existing corridor-wide ramp metering algorithms are able to take the position.

The corridor-wide ramp metering algorithms, also known as coordinated ramp metering algorithm, take into account sections of the freeway including multiple on-ramp and off-ramp as unitary dynamic systems, instead of calculating each local on-ramp inflow rate independently. Therefore, more macroscopic control of the traffic can be achieved.

In this study, the corridor-level control algorithm is designed via the idea of the Next Generation Stratified Ramp Metering Algorithm proposed by Geroliminis et al [25]. The basic objectives of the algorithm are to balance the ramp waiting time and ramp inflow rate, namely, the demand and queue lengths at on-ramps and the level of congestion on the mainline, to delay the operation of the breakdown and to accelerate system recovery.

Instead of the traditional layer-based algorithm, which fixed the control zone, the proposed approach dynamically determines the zones in real time based on the current traffic condition. The zone is defined as a segment of the freeway consisting of multiple consecutive sections, which is a sub-segment of the freeway between two consecutive mainline detector locations (in traditional freeway system). For each section, the congestion threat index, marked as 0, 1, and 2, will be calculated to identify the severity of each potential bottleneck. Level 2 congestion threat index of a section indicates a location that is already congested, level 0 of a section

indicates a location that has minimal threat to be congested, and level 1 is a state in between. The detailed approach to calculate the indices refers to [25]. After that, the controlled ramp can be identified via the indices' information. Each zone has only one controlled ramp located at the most downstream end. Figure 5 depicts the flow chart to identify the controlled ramp.
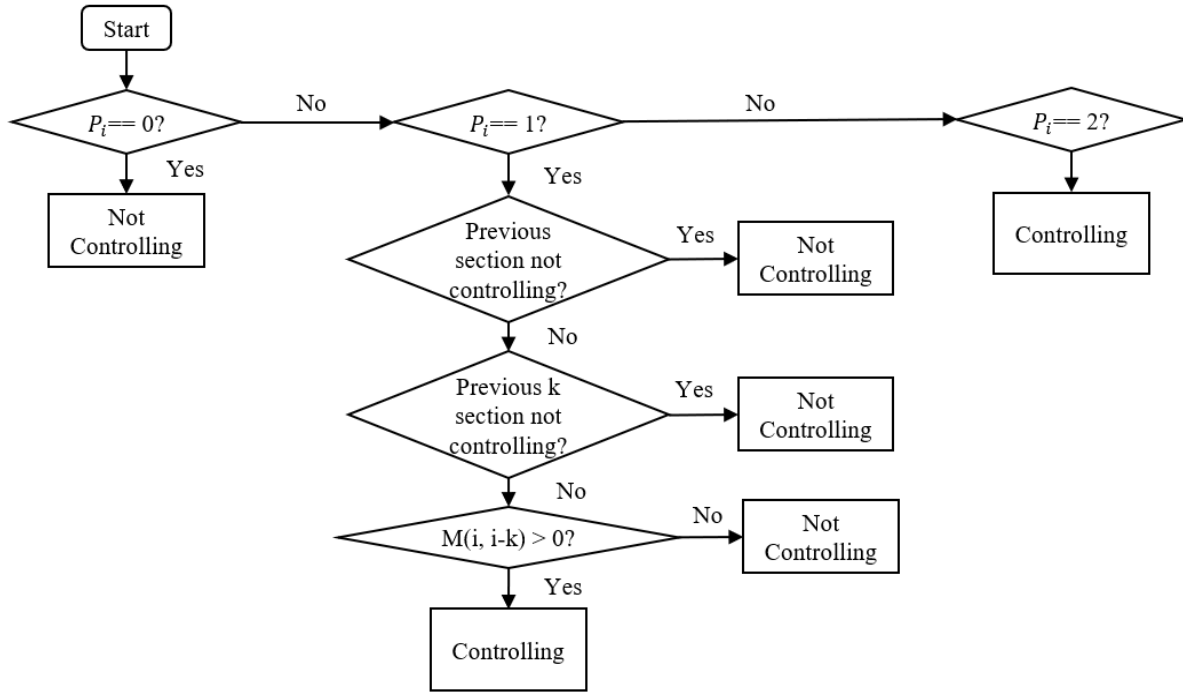
where i in current section ID; k is number of consecutive downstream section; P_i is the congestion threat index of the current section; $M(i, i-k)$ is the net inflow between the two locations i and $i-k$, defined as the sum of on-ramp volumes minus the sum of off-ramp volumes plus the capacity flow difference for all ramps between the two locations.

Figure 5. Flowchart of next generation stratified ramp metering algorithm [25].

Then, with the zone identification information, the metering actions matrix is defined in the following Table 1.

Table 1. Conditions to estimate the suggested ramp inflow rate.

Condition	Index=0, downstream not controlled ramp	Index=0/1, downstream controlled ramp	Index=1, downstream not controlled ramp	Index=2
Type	Uncongested Ramp Metering	Controlled Ramp Metering	Controlled Ramp Metering	Congested Ramp Metering
Suggested Ramp Inflow Rate	$c^h(i) - q(i)$	$d_i - \dfrac{\Delta t_i d_i \left[d_j - r_t(j) \right]}{\Delta t_j d_j}$	$r_{t-1}(i)$ $-K_1(T_t^w(i) - \tau_w)$ $+K_2 T_t^k(i),$	$r_{t-1}(i) + K_1 T_t^w(i),$ if $T_t^w(i) < 0$ $r_{t-1}(i) + K_2 T_t^k(i),$ otherwise

where $c^h(i)$ is the uncongested capacity; q(i) is the mainline demand; d_i the ramp demand; j is the downstream controlling ramp id; $r_t(j)$ is the current suggested metering rate of location j; $\Delta t_i = T_{crit} - w_t(i)$, where T_{crit} is the ramp delay constraint and $w_t(i)$ is the current maximum waiting time at ramp i; K_1 and K_2 are contribution parameters depicting the importance of breakdown on ramp and on mainline; τ_w is the safe time-to-breakdown defined for the ramp; $T_t^w(i)$ and $T_t^k(i)$ are the estimated time remaining to congestion on the mainline and ramp. The values of the parameters and the variables are calculated based on historical or real-time data.

Involved Vehicle Identification

The buffer zone is designed to differentiate the involved vehicles within each control decision cycle for online implementation. As aforementioned, the length of on-ramp buffer zone is predefined, while the length of the mainline buffer zone may change with the traffic condition, which is considered as

$$L_{main} = \frac{q_{main}}{q_{suggested}} n / d_{main} \tag{4}$$

where q_{main} is the mainline traffic flow known from corridor traffic condition; $q_{suggested}$ is the suggested on-ramp inflow rate assumed to be known; n is the number of on-ramp vehicles currently in the buffer zone; d_{main} is the mainline density. The vehicles in the buffer zones of both on-ramp and mainline would be controlled as a whole set till their travel through the merging area within the same control decision cycle. Until another vehicle reaches the downstream boundary of on-ramp buffer zone, a new control decision cycle is initiated and a new set of involved vehicles are determined. Depending on the prevailing traffic conditions, the

NCST

number of involved vehicles in each set (during each control decision cycle) may vary and the control processes or multiple LQ tracker controllers for different vehicle sets may perform in parallel.

Optimal Sequence Determination

There are three sub-steps in the *Optimal Sequence Determination* process, including possible sequence generation, linear quadratic tracking, and energy consumption estimation. In this process, all the possible orders of the involved vehicles will first be generated. For each order, the optimal system inputs (acceleration of each involved vehicle) can be solved by a LQ tracker. Then based on the system dynamics, the speed profile can be calculated and the energy consumption can be estimated by a microscopic electric vehicle energy consumption model [3]. Each possible order is associated with one aggregated energy consumption value (for all the involved vehicles), and the sequence with the least aggregated energy consumption is picked as the optimal scenario. Vehicle-level will then use this order to control the vehicles motion.

1) ***Possible sequence generation***: Given the assumption that all the involved vehicles within each control decision cycle would not change their lanes during the merging process, vehicles on the same lane cannot overpass their preceding ones. Therefore, if there are M mainline vehicles and N on-ramp vehicles, the number of possible sequences after merging equals to $P(M + N, N)$, where $P(\cdot)$ is the permutation operation. Because a large number of involved vehicles may lead to combinatorial explosion and make the system intractable for real-time implementation, the predefined length of on-ramp buffer zone plays a key role to confine the control group to a reasonable scale. This can be considered as one way to balance the computational load.

2) ***Linear quadratic tracking***: Based on the initial states, the finite-horizon linear quadratic tracking algorithm is able to generate the optimal solution in the designated finite time. The weight Q and R matrices are fine tuned to keep the balance of tracking error and control input and also to hold the hard constraints. For better performance, the weighting factors for on-ramp vehicles and for those mainline vehicles are tuned independently. The solution is calculated iteratively as follows:

$$\begin{cases} S_N = C^T Q_N C \\ V_N = C^T Q_N r_N \end{cases} \tag{5}$$

$$\begin{cases} S_i = C^T Q C + A^T S_{i+1} - S_{i+1} B (R + B^T S_{i+1} B)^{-1} B^T S_{i+1} A \\ V_i = \{A^T - A^T S_{i+1} B (R + B^T S_{i+1} B)^{-1} B^T\} V_{i+1} + C^T Q r_i \end{cases} \quad \forall i = 1, 2 \dots, N-1 \tag{6}$$

$$\begin{cases} K_i = (B^T S_{i+1} B + R)^{-1} B^T S_{i+1} A \\ K_i^v = (B^T S_{i+1} B + R)^{-1} B^T \end{cases} \quad \forall i = 1, 2 \dots, N-1 \tag{7}$$

where Equation (6) is the discrete time algebraic Riccati equation; N is the predefined finite horizon; i is the time index for each iteration; K_i is the feedback gain and K_i^v is the feed-forward gain. $S_i, V_i, K_i,$ and K_i^v are found iteratively backwards in time. Then the

solution is given by $\mu_i = -K_i x_k + K_i^v V_i$. With the control input μ_i and the system dynamic Eqution (2), trajectories of all the vehicles can be calculated.

3) **Energy consumption estimation**: Based on the electric vehicle energy consumption estimation model, the energy consumption rate can be determined by the nonlinear function of current speed and acceleration:

$$P = f(v, a) = f_0 + l_1 v\cos(\alpha) + l_2 v\sin(\alpha) + l_3 v^3 + l_4 va + l_5 v^2\cos(\alpha) + l_6 v^2\sin(\alpha) + l_7 v^4 + l_8 v^2 a \tag{8}$$

where l_i is the model parameter calibrated by different driving conditions; α is the road grade (rad). In our simulation, we assume the road grade is zero.

Optimal Motion Control

This module uses the results from previous step to control the motion of the involved vehicles. The controller chosen in this study is a receding-horizon LQ tracker for potentially online implementation. The advantage of receding-horizon LQ tracker than the previous finite-horizon LQ tracker is that it enables the closed-loop mechanism in the control system. At each rolling time window, the controller can update the initial states with the current state, and we only use the converged feedback gain and feed-forward gain to control the system. The Q and R parameters for this receding-horizon controller are selected to be the same as the ones used in the prediction step to get consistent results. When the constraints do not hold in certain time step, the optimal solution will be recalculated by enlarging the current time window until the constraints are satisfied.

As aforementioned, given the suggested ramp inflow rate, not all the vehicles within the on-ramp buffer zone should be controlled to enter the merging zone during the same time interval. Under the selected car-following model, if the leader arrives the trigger point earlier than this time, the ramp inflow rate would be higher than suggested. Here, we further assume the following behavior of the leader (to its predecessor if any) can be modeled by IDM [76], based on which we predict its ETA. The vehicle governed by the IDM presents a second order dynamic shown as follow:

$$\dot{v} = a\left(1 - \left(\frac{v}{v_0}\right)^\delta - \left(\frac{s^*(v - \Delta v)}{s}\right)^2\right) \tag{9}$$

$$s^*(v - \Delta v) = s_0 + vT + \frac{v\Delta v}{2\sqrt{ab}} \tag{10}$$

where v_0 is desired velocity; s_0 is minimum spacing; T is the desired time headway; a is the maximum vehicle acceleration; b is comfortable braking deceleration. The leader will be controlled by a linear feedback controller if ETA is smaller than the suggested time.

Simulation Study

In this chapter, we focus on the simulation study for the proposed ramp merging system with the microscopic traffic simulator PTV VISSIM [78] to validate the effectiveness of the system. Different from the numerical simulation that most of the previous research conducted, traffic simulation can offer more realistic real-time interaction between the equipped vehicles and other traffic in the network. This enables a better observation of the impact of the proposed system on the whole traffic over the time. Through the DriverModel API, the behavior of the CAEVs in the network can be controlled with the proposed algorithms. Uncontrolled vehicles in the network are modeled by the default vehicle model in VISSIM. The simulation network is built based on a segment along California State Route 91 (SR-91), including the Serfas Club Dr. on-ramp and Paseo Grande on-ramp in Corona, CA (see Figure 6). We conduct simulation study on both single-ramp network (with the Serfas Club Dr. on-ramp only) and two-ramp network, respectively, and the results are presented in the following sections. As our project is focused on the longitudinal control of the vehicles, we simplify the mainline segment with single lane.

Figure 6. Snapshot of simulation network in PTV VISSIM.

Simulation with Single-Ramp Network

In the single-ramp (i.e., Serfas Club Dr. on the left side of the figure) network simulation, the conventional ramp metering system and the ramp without any control approach are also introduced for comparison. Based on the observation and parameter settings, the merging area capacity is around 1800 passenger car unit/hour/lane (pcu/hr/ln). According to this, the ramp inflow rate is dynamically adjusted to regulate the overall traffic flow not to exceed the capacity. For fair comparison, the baseline ramp metering rate is also set to match the inflow rate that is regulated by the proposed system. The desired speed for mainline/merging traffic is 73.8 mph. The initial speed of on-ramp vehicles while entering the control zone is 33.5 m/s.

We consider two scenarios based on different traffic conditions. Each scenario contains two phases, lasting 600s respectively. For mainline traffic, 1600 pcu/hr/ln is considered as heavy, and 1200 pcu/hr/ln is as moderate. For ramp traffic, 500 pcu/hr/ln is considered as heavy, and 300 pcu/hr/ln is as moderate. Table 2 shows the settings of simulation scenarios in this study.

Table 2. Scenario matrix for the single-ramp network simulation.

	Phase 1: 0-600s		Phase 2: 600-1200s	
	Mainline Inflow	Ramp Inflow	Mainline Inflow	Ramp Inflow
Scenario 1	1600	500	1200	300
Scenario 2	1600	300	1200	500

The simulation results measured by the mobility metric are shown in Table 3 and Table 4. The mobility performance is measured by network efficiency,

$$Q = \frac{VMT}{VHT}$$

where *VMT* is the total vehicle-miles traveled in the network; and *VHT* is the total vehicle-hours traveled in the network accordingly.

In Scenario 1, the heavy traffic of both mainline and ramp in Phase 1 rapidly caused the congestion in the network for both ramp metering case and no control case. At each time when the ramp vehicle merged, a shockwave was generated and spread to the upstream, which eventually evolved to stop-and-go traffic along the mainline. In addition, the consistent shockwaves impeded the recovery of congestion, which led to low mobility of the network. As shown in Table 3, the overall mobility of no control case has only 29.6 mph. Although ramp vehicles have relatively high mobility, their uncooperative behaviors severely influenced the mainline vehicles. Interestingly, even though the traffic experienced severe stop-and-go situations with very low average speed or network efficiency, the system energy consumption (in kWh per 100 mile) is decent. A hypothesis is that electric vehicles may operate efficiently in terms of energy consumption under relatively congested scenarios due to their regenerative braking feature [79]. On the other hand, in the ramp metering case, since the ramp inflow rate was regulated, less significant impact was involved on the mainline. The mainline mobility in this case was 57.9 mph, much better than the no control case. However, the ramp metering operation severely limited the mobility on ramp, and the extremely high frequency of stop-and-go maneuvers at very low speed also caused significant energy waste for electric vehicles. As to the case of the proposed optimal control, the cooperation led to the highest overall mobility (including both mainline and ramp), which is improved by 43.1% and 102.0%, respectively, compared to the ramp metering case and no control case. In terms of energy consumption, the proposed system outperformed both the ramp metering case and the no control case for ramp traffic with the smoothing effects, but the mainline traffic consumed more energy mainly due to the high speed (thus high load for EVs) to be maintained.

Table 3. Simulation results of mobility and energy for scenario 1 (single-ramp).

		Mobility (mph)	Energy (kWatt/100 mile)
Optimal Control	Overall	59.8	48.84
	Mainline	62.1	50.67
	Ramp	48.3	37.26
Ramp Metering	Overall	41.8	51.34
	Mainline	57.9	47.15
	Ramp	13.6	82.84
No Control	Overall	29.6	44.13
	Mainline	27.6	43.95
	Ramp	52.2	45.43

In Scenario 2 (see Table 4), since the heavy traffic of mainline and ramp were staggered, the traffic condition was generally moderate compared to Scenario 1. Therefore, the mobility performance is better for all cases. The proposed optimal control system still achieved the best mobility, improving 45.3% compared to the ramp metering case and 95.6% compared to the no control case. In terms of energy consumption, high average speed resulted from the proposed system seems to be a penalty for electric vehicles, and the "sweet spot" (in terms of energy factor) in this study falls in the range between 27 mph and 34 mph.

Table 4. Simulation results of mobility and energy for scenario 2 (single-ramp).

		Mobility (mph)	Energy (kWatt/100 mile)
Optimal Control	Overall	66.7	51.53
	Mainline	69.0	53.29
	Ramp	54.1	39.58
Ramp Metering	Overall	45.9	50.97
	Mainline	64.5	46.93
	Ramp	14.5	81.29
No Control	Overall	34.1	42.87
	Mainline	32.7	42.59
	Ramp	49.6	44.95

Simulation with Two-Ramp Network

In this section, the cooperation of two on-ramp (i.e., Serfas Club Dr. and Paseo Grande from left to right, as defined below as ramp 1 and ramp 2, respectively) is considered. The two-phase test scenario is described in Table 5.

Table 5. Test scenario for the two-ramp network simulation.

Phase 1: 0-600s			Phase 2: 600-1200s		
Mainline Inflow	Ramp 1 Inflow	Ramp 2 Inflow	Mainline Inflow	Ramp 1 Inflow	Ramp 2 Inflow
1200	500	200	1200	300	200

The simulation results are summarized in Table 6. Similar to the single ramp scenarios, congestion happened at both ramp in phase 1 for the no control case. The congestion spread to the upstream and severely influenced the mobility of the mainline vehicles. Therefore, the mainline mobility is as low as 30.0 mph. The mobility of ramp 1 vehicles was lower than the ramp 2 vehicles mainly because that after merging into the mainline, ramp 1 vehicle would slow down by the shockwaves generated from ramp 2. For the ramp metering case, mobility of ramps was sacrificed to reduce the influence on the mainline. As the result, on major shockwave was observed while simulation, and the mainline's mobility increasing 114.7% and the overall mobility increasing 21.0% compared to the no control case. While it consumed 28.3% more energy than the no control case, because of the stop-and-go maneuver of on-ramp vehicles. As to the proposed optimal control case, the smoothest vehicles' trajectory was provided. Therefore, highest mobility (mph) was given, improving 56.5% compared to the ramp metering case and 89.4% compared to the no control case. What's more, the energy consumption of the optimal control case is 12.5% less than the ramp metering case and 12.3% more than no control case.

Table 6. Simulation results of mobility and energy for two-ramp network.

		Mobility (mph)	Energy (kWatt/100 mile)
Optimal Control	Overall	62.3	47.13
	Mainline	65.3	48.54
	Ramp 1	57.3	44.91
	Ramp 2	54.0	40.09
Ramp Metering	Overall	39.8	53.84
	Mainline	64.4	47.76
	Ramp 1	17.1	73.68
	Ramp 2	52.0	52.72
No Control	Overall	32.9	41.98
	Mainline	30.0	42.64
	Ramp 1	41.8	38.79
	Ramp 2	57.5	46.32

Conclusions and Future Work

In this project we proposed a hierarchical ramp merging system for Connected and Automated Electric Vehicles (CAEVs). The system can not only cooperate the vehicles at ramp merging area to achieve a safer, smoother, and more efficient traffic flow, but also be able to regulate ramp vehicles' inflow rate which has the potential to leverage the corridor-wise efficiency by integrating with effective perimeter control on multiple ramps. We utilized the SRM algorithm for corridor level ramp inflow rate calculation. And we developed ramp-level data collection logic that can determine the right set of vehicles for online control and collect the associated information based on the prevailing traffic conditions. Unlike most existing studies using simple sequencing protocol (e.g., first-come-first-serve), we used a finite linear Quadratic (LQ) tracker to identify the optimal merging sequence in terms of energy consumption. A receding horizon LQ tracker with the same parameters was used for the optimal motion control. The simulation results verified the effectiveness of the proposed system. It should be pointed out that such multi-stage optimization framework tries to balance the problem simplification and system optimality. It cannot theoretically guarantee the global optimal solution to system-wide efficiency.

An ongoing research direction is to investigate the eco-ramp control strategy for gasoline or diesel powered vehicles whose energy/fuel estimation models are more complicated than the electric vehicles used in this study. In addition, the application to mixed traffic scenarios where legacy vehicles, connected only vehicles, and CAVs co-exist would be one of our future steps.

NCST

References

1. R. E. Fenton, "Automatic vehicle guidance and control—a state of the art survey," IEEE Transactions on Vehicular Technology, vol. 19, no. 1, pp. 153–161, February1970.

2. J. Rios-Torres and A. A. Malikopoulos, "Automated and Cooperative Vehicle Merging at Highway On-Ramps," IEEE Trans. Intell. Transp. Syst., vol. 18, no. 4, pp. 780–789, 2017.

3. F. Ye, G. Wu, K. Boriboonsomsin, and M. J. Barth, "A hybrid approach to estimating electric vehicle energy consumption for ecodriving applications," in 2016 IEEE 19th International Conference on Intelligent Transportation Systems, 2016, pp. 719–724.

4. K. Shaaban, M. A. Khan, and R. Hamila, "Literature Review of Advancements in Adaptive Ramp Metering," Procedia Computer Science, vol. 83, no. Ant, pp. 203–211, 2016.

5. W. Jin and M. Zhang, "Evaluation of On-ramp Control Algorithims," California Partners for Advanced Transit and Highways, 2001.

6. K. Bogenberger and A. D. May, "Advanced Coordinated Traffic Responsive Ramp Metering Strategies," California PATH, Final Report, 1999.

7. L. Jacobson, K. Henry, and O. Mehyar, "Real-time metering algorithm for centralized control," Transportation Research Record, no. 1732, pp. 20–32, 1989.

8. G. Paesani, J. Kerr, P. Perovich, and F. E. Khosravi, "System-Wide Adaptive Ramp Metering (SWARM)," Merging the Transportation and Communications Revolutions. Abstracts for ITS America Seventh Annual Meeting and Exposition, 1997.

9. Y. Stephanedes, "Implementation of on-line zone control strategies for optimal ramp metering in the Minneapolis ring road," Road Traffic Monitoring and Control, vol. 26-28, pp. 181–184, 1994.

10. C. Taylor, D. Meldrum, and L. Jacobson, "Fuzzy ramp metering: Design overview and simulation results," Transportation Research Record, no. 1634, pp. 10–18, 1998.

11. C. Taylor and D. Meldrum, "Evaluation of a Fuzzy Logic Ramp Metering Algorithm: a Comparative Study Among Three Ramp Metering Algorithms," Washington State Department of Transportation, Technical Report, February, 2000.

12. J.-C. Liu, J. L. Kim, Y. Chen, Y. Hao, S. Lee, T. Kim, and M. Thomadakis, "An Advanced real-time ramp metering system (ARMS): the system concept," Texas Department of Transportation, Texas, Technical Report, November, 1994.

13. O. J. Chen, A. F. Hotz, and M. E. Ben-Akiva, "Development and Evaluation of a Dynamic Ramp Metering Control Model," IFAC Transportation Systems, 1997.

14. M. Papageorgiou, H. Hadj-Salem, and J. Blosseville, "ALINEA: A local feedback control law for on-ramp metering," Transportation Research Record, pp. 58–64, 1991.

15. M. Papageorgiou, E. Kosmatopoulos, I. Papamichail, and Y. Wang, "A misapplication of the local ramp metering strategy ALINEA," IEEE Transactions on Intelligent Transportation Systems, vol. 9, no. 2, pp. 360–365, June 2008.

16. M. Papageorgiou, H. Hadj-Salem, J. Blosseville, and N. Bhouri, "Modelling and Real-time Control of Traffic Flow on the Boulevard Peripherique in Paris," Transportation Research Part A: General, vol. 24, pp. 345–359, 1990.

17. E. Smaragdis, M. Papageorgiou, and E. Kosmatopoulos, "A flowmaximizing adaptive local ramp metering strategy," Transportation Research Part B: Methodological, vol. 38, no. 3, pp. 251–270, 2004.

18. R. Jiang, E. Chung, and J. Lee, "Local On-ramp Queue Management Strategy with Mainline Speed Recovery," Procedia-Social and Behavioral Sciences, vol. 43, pp. 201–209, 2012.

19. Y. Kan, Y. Wang, M. Papageorgiou, and I. Papamichail, "Local ramp metering with distant downstream bottlenecks: A comparative study," Transportation Research Part C: Emerging Technologies, vol. 62, pp. 149–170, January 2016.

20. I. Papamichail, M. Papageorgiou, V. Vong, and J. Gaffney, "HERO coordinated ramp metering implemented at the Monash Freeway," Transportation Research Board, 89th Annual Meeting, Washington, DC, pp. 10–14, 2010.

21. L. Isaksen and H. Payne, "Suboptimal control of linear systems by augmentation with application to freeway traffic regulation," IEEE Transactions on Automatic Control, vol. 18, no. 3, pp. 210–219, June 1973.

22. N. Goldstein and K. Kumar, "A decentralized control strategy for freeway regulation," Transportation Research Part B: Methodological, vol. 16, no. 4, pp. 279–290, August 1982.

23. A. Hegyi, B. De Schutter, and H. Hellendoorn, "Model predictive control for optimal coordination of ramp metering and variable speed limits," Transportation Research Part C: Emerging Technologies, vol. 13, no. 3, pp. 185–209, June 2005.

24. J. Haddad, M. Ramezani, and N. Geroliminis, "Cooperative traffic control of a mixed network with two urban regions and a freeway," Transportation Research Part B: Methodological, vol. 54, pp. 17–36, August 2013.

25. N. Geroliminis, A. Srivastava, and P. Michalopoulos, "Development of the Next Generation Stratified Ramp Metering Algorithm Based on Freeway Design," Center for Transportation Studies. Retrieved from the University of Minnesota Digital Conservancy, Tech. Rep., 2011.

26. N. Geroliminis, J. Haddad, and M. Ramezani, "Optimal perimeter control for two urban regions with macroscopic fundamental diagrams: A model predictive approach," IEEE Transactions on Intelligent Transportation Systems, vol. 14, no. 1, pp. 348–359, 2013.

27. H. M. Zhang and S. G. Ritchie, "Freeway ramp metering using artificial neural networks," Transportation Research Part C: Emerging Technologies, vol. 5, no. 5, pp. 273–286, 1997.

28. C. Wei and K. Wu, "Applying an artificial neural network model to freeway ramp metering control," Transportation Planning Journal, vol. 25, no. 3, 1996.

29. C. Lu and J. Huang, "A self-learning system for local ramp metering with queue management," Transportation Planning and Technology, vol. 40, no. 2, pp. 182–198, 2017.

30. A. Fares and W. Gomaa, "Multi-Agent Reinforcement Learning Control for Ramp Metering," in Progress in Systems Engineering. Springer, 2015, pp. 167–173.

31. C. Lu, J. Huang, L. Deng, and J. Gong, "Coordinated Ramp Metering with Equity Consideration Using Reinforcement Learning," Journal of Transportation Engineering, Part A: Systems, 2017.

32. F. Belletti, D. Haziza, G. Gomes, and A. M. Bayen, "Expert Level Control of Ramp Metering Based on Multi-Task Deep Reinforcement Learning," IEEE Transactions on Intelligent Transportation Systems, vol. 19, no. 4, pp. 1198–1207, 2018.

33. T. Schmidt-Dumont and J. H. Van Vuuren, "Decentralised reinforcement learning for ramp metering and variable speed limits on highways," IEEE Transactions on Intelligent Transportation Systems, vol. 14, no. 8, 2015.

34. J. Rios-Torres and A. A. Malikopoulos, "A survey on the coordination of connected and automated vehicles at intersections and merging at highway on-ramps," IEEE Transactions on Intelligent Transportation Systems, vol. 18, no. 5, pp. 1066–1077, May 2017.

35. R. Scarinci and B. Heydecker, "Control concepts for facilitating motorway on-ramp merging using intelligent vehicles," Transport Reviews, vol. 34, no. 6, pp. 775–797, 2014.

36. G. K. Schmidt and B. Posch, "A two-layer control scheme for merging of automated vehicles," in The 22nd IEEE Conference on Decision and Control, Dec 1983, pp. 495–500.

37. B. Ran, S. Leight, and B. Chang, "A microscopic simulation model for merging control on a dedicated-lane automated highway system," Transportation Research Part C: Emerging Technologies, vol. 7, no. 6, pp. 369–388, 1999.

38. T. Awal, L. Kulik, and K. Ramamohanrao, "Optimal traffic merging strategy for communication- and sensor-enabled vehicles," in 16th International IEEE Conference on Intelligent Transportation Systems (ITSC 2013), Oct 2013, pp. 1468–1474.

39. G. Raravi, V. Shingde, K. Ramamritham, and J. Bharadia, "Merge algorithms for intelligent vehicles," in Next Generation Design and Verification Methodologies for Distributed Embedded Control Systems, S. Ramesh and P. Sampath, Eds. Dordrecht: Springer Netherlands, 2007, pp. 51–65.

40. Y. Xie, H. Zhang, N. H. Gartner, and T. Arsava, "Collaborative merging strategy for freeway ramp operations in a connected and autonomous vehicles environment," Journal of Intelligent Transportation Systems, vol. 21, no. 2, pp. 136–147, 2017

41. A. Uno, T. Sakaguchi, and S. Tsugawa, "A merging control algorithm based on inter-vehicle communication," in Proceedings 199 IEEE/IEEJ/JSAI International Conference on Intelligent Transportation Systems, Oct. 1999, pp. 783–787.

42. X.-Y. Lu and K. J. Hedrick, "Longitudinal control algorithm for automated vehicle merging," in Proceedings of the 39th IEEE Conference on Decision and Control, vol. 1, Dec. 2000, pp. 450–455.

43. T. Dao, C. M. Clark, and J. P. Huissoon, "Distributed platoon assignment and lane selection for traffic flow optimization," in IEEE Intelligent Vehicles Symposium (IV), Jun. 2008, pp. 739–744.

44. Y. Zhou, M. E. Cholette, A. Bhaskar, and E. Chung, "Optimal vehicle trajectory planning with control constraints and recursive implementation for automated on-ramp merging," IEEE Transactions on Intelligent Transportation Systems, pp. 1–12, 2018.

45. Z. Wang, G. Wu, and M. Barth, "Distributed consensus-based cooperative highway on-ramp merging using V2X communications," in SAE Technical Paper, April 2018.

46. Z. Wang, G. Wu, K. Boriboonsomsin, M. J. Barth, K. Han, B. Kim, and P. Tiwari, "Cooperative ramp merging system: Agent-based modeling and simulation using game engine," SAE International Journal of Connected and Automated Vehicles, vol. 2, no. 2, pp. 115–128, 2019.

47. T. Seo, A. M. Bayen, T. Kusakabe, and Y. Asakura, "Traffic state estimation on highway: A comprehensive survey," Annual Reviews in Control, vol. 43, pp. 128–151, January 2017.

48. B. Greenshields, J. Bibbins, W. Channing, and H. Miller, "A study of traffic capacity," Highway Research Board proceedings, vol. 1935, 1935.

49. G. Newell, "A simplified theory of kinematic waves in highway traffic, Part I: General theory," Transportation Research Part B: Methodological, vol. 27, no. 4, pp. 281–287, 1993.

50. C. F. Daganzo, "The cell transmission model: A dynamic representation of highway traffic consistent with the hydrodynamic theory," Transportation Research Part B: Methodological, vol. 28, no. 4, pp. 269–287, 1994.

51. M. Lighthill and G. Whitham, "On kinematic waves II. A theory of traffic flow on long crowded roads," Proceedings of the Royal Society of London. Series A. Mathematical and Physical Sciences, vol. 229, no. 1178, pp. 317–345, May 1955.

52. P. I. Richards, "Shock Waves on the Highway," Operations Research, vol. 4, no. 1, pp. 42–51, February 1956.

53. H. Payne, "Models of freeway traffic and control," Mathematical Models of Public Systems, no. 1, pp. 51–61, 1971.

54. G. Whitham, "Linear and nonlinear waves," John Wiley & Sons, 1974.

55. B. Coifman, "Estimating travel times and vehicle trajectories on freeways using dual loop detectors," Transportation Research Part A: Policy and Practice, vol. 36, no. 4, pp. 351–364, 2002.

56. Y. Wang and M. Papageorgiou, "Real-time freeway traffic state estimation based on extended kalman filter: a general approach," Transportation Research Part B: Methodological, vol. 39, no. 2, pp. 141–167, 2005.

57. S. Tak, S. Woo, and H. Yeo, "Data-driven imputation method for traffic data in sectional units of road links," IEEE Transactions on Intelligent Transportation Systems, vol. 17, no. 6, pp. 1762–1771, June 2016.

58. R. Florin and S. Olariu, "On a variant of the mobile observer method," IEEE Transactions on Intelligent Transportation Systems, vol. 18, no. 2, pp. 441–449, February 2017.

59. N. Bekiaris-Liberis, C. Roncoli, and M. Papageorgiou, "Highway traffic state estimation with mixed connected and conventional vehicles," IEEE Transactions on Intelligent Transportation Systems, vol. 17, no. 12, pp. 3484–3497, December 2016.

60. M. Brackstone and M. McDonald, "Car-following: a historical review," Transportation Research Part F: Traffic Psychology and Behaviour, vol. 2, no. 4, pp. 181–196, 1999.

61. M. Saifuzzaman and Z. Zheng, "Incorporating human-factors in car-following models: A review of recent developments and research needs," Transportation Research Part C: Emerging Technologies, vol. 48, pp. 379–403, 2014.

62. P. Gipps, "A behavioural car-following model for computer simulation," Transportation Research Part B: Methodological, vol. 15, no. 2, pp. 105–111, 1981.

63. S. Krauss, "Microscopic modeling of traffic flow: Investigation of collision free vehicle dynamics," Ph.D. dissertation, 1998.

64. M. Treiber, A. Hennecke, and D. Helbing, "Derivation, properties, and simulation of a gas-kinetic-based, non-local traffic model," 1999.

65. S. Panwai and H. Dia, "Comparative evaluation of microscopic car-following behavior," IEEE Transactions on Intelligent Transportation Systems, vol. 6, no. 3, pp. 314–325, Sept. 2005.

66. G. han Peng and R. jun Cheng, "A new car-following model with the consideration of anticipation optimal velocity," Physica A: Statistical Mechanics and its Applications, vol. 392, no. 17, pp. 3563–3569, 2013.

67. J. M. and, "An anfis controller for the car-following collision prevention system," IEEE Transactions on Vehicular Technology, vol. 50, no. 4, pp. 1106–1113, July 2001.

68. A. Khodayari, A. Ghaffari, R. Kazemi, and R. Braunstingl, "A modified car-following model based on a neural network model of the human driver effects," IEEE Transactions on Systems, Man, and Cybernetics-Part A: Systems and Humans, vol. 42, no. 6, pp. 1440–1449, November 2012.

69. F. Wu and D. B. Work, "Connections between classical car following models and artificial neural networks," in 2018 21st International Conference on Intelligent Transportation Systems (ITSC), Nov 2018, pp. 3191–3198.

70. V. Kanagaraj, G. Asaithambi, C. N. Kumar, K. K. Srinivasan, and R. Sivanandan, "Evaluation of different vehicle following models under mixed traffic conditions," Procedia - Social and Behavioral Sciences, vol. 104, pp. 390–401, 2013, 2nd Conference of Transportation Research Group of India (2nd CTRG).

71. G. Agamennoni, J. I. Nieto, and E. M. Nebot, "A bayesian approach for driving behavior inference," in 2011 IEEE Intelligent Vehicles Symposium (IV), June 2011, pp. 595–600.

72. J. Morton, T. A. Wheeler, and M. J. Kochenderfer, "Analysis of recurrent neural networks for probabilistic modeling of driver behavior," IEEE Transactions on Intelligent Transportation Systems, vol. 18, no. 5, pp. 1289–1298, May 2017.

73. F. Ye, P. Hao, X. Qi, G. Wu, K. Boriboonsomsin, and M. J. Barth, "Prediction-based eco-approach and departure at signalized intersections with speed forecasting on preceding vehicles," IEEE Transactions on Intelligent Transportation Systems, vol. 20, no. 4, pp. 1378–1389, April 2019.

74. A. Ghaffari, A. Khodayari, A. Panahi, and F. Alimardani, "Neural network-based modeling and prediction of the future state of a stop-and-go behavior in urban areas," in 2012 IEEE International Conference on Vehicular Electronics and Safety (ICVES 2012), July 2012, pp. 399–404.

75. T. Toledo, H. N. Koutsopoulos, and M. Ben-Akiva, "Integrated driving behavior modeling," Transportation Research Part C: Emerging Technologies, vol. 15, no. 2, pp. 96–112, 2007.

76. A. Kesting, M. Treiber, and D. Helbing, "Enhanced intelligent driver model to access the impact of driving strategies on traffic capacity," Philos. Trans. R. Soc. A Math. Phys. Eng. Sci., vol. 368, no. 1928, pp. 4585–4605, 2010.

77. S. Cui, B. Seibold, R. Stern, and D. B. Work, "Stabilizing traffic flow via a single autonomous vehicle: Possibilities and limitations," in 2017 IEEE Intelligent Vehicles Symposium (IV), June 2017, pp. 1336–1341.

78. PTV VISSIM. PTV Group, accessed on September 27th, 2019. [Online]. Available: http://vision-traffic.ptvgroup.com/en-us/products/ptv-vissim/

79. Ehsani, M., Y. Gao, and A. Emadi (2010). "Modern Electric, Hybrid Electric, and Fuel Cell Vehicles: Fundamentals, Theory, and Design (2nd Edition)". Taylor and Francis

Data Management

Products of Research

In this project, we collected vehicles' characteristics and trajectory data from the microscopic traffic simulator, PTV VISSIM. These data were used for evaluating the performance of the proposed ramp control algorithm.

Data Format and Content

The data are output from PTV VISSIM via application programming interfaces (APIs). The files are in .csv format. The contents of each file include vehicle ID, vehicle type (to differentiate if the vehicle is spawned from mainline, ramp 1 or ramp 2), vehicle speed (in m/s), traveled distance from the spawning (i.e., odometer reading in meter), and energy consumption for connected and automated electric vehicles (in KJ) on the basis of one simulation time step (10 Hz).

Data Access and Sharing

The data are made available publicly via the UC Riverside instance of DataDRYAD: https://datadryad.org/stash, which is licensed under a CC0 1.0 Universal (CC0 1.0) Public Domain Dedication license. The DOI for the dataset is https://doi.org/10.6086/D10M3D.

Reuse and Redistribution

The data should be restricted for research use only. If the data are used, our work should be properly cited: Wu, Guoyuan; Zhao, Zhouqiao (2019), PTV VISSIM Simulation Data for Efficient Eco-Ramp Control Project Funded by NCST 18-19, UC Riverside, Dataset, https://doi.org/10.6086/D10M3D.